Acta Metallurgica, Vol. 28, pp. 1301 to 1313

0001-6160/80/0901-1301$02.00/0

THE SEQUENCE OF PRECIPITATION IN Cu–2$^{w}/_{o}$ Be ALLOYS

R. J. RIOJA and D. E. LAUGHLIN

Metallurgy and Materials Science Department, Carnegie-Mellon University, Pittsburgh, Pennsylvania 15213 U.S.A.

(*Received* 11 *September* 1979)

Abstract—We present herein a summary of the morphologies and TEM diffraction effects of the several metastable phases observed when a supersaturated Cu–2$^{w}/_{o}$ Be alloy decomposes at temperatures ranging from 500°C (773 K) to room temperature. These observations are correlated with previously recorded ones and a consistent nomenclature of the metastable phases is given. A metastable equiaxed phase has been found to form prior to the well-known plate-like G.P. zones. Also the sequence of precipitation is recorded as a function of temperature and quenching method. The results are discussed in terms of nucleation theory.

Résumé—Nous présentons ici un résumé des morphologies et des effets de diffraction électronique des diverses phases métastables que l'on observe lorsqu'un alliage Cu–2% Be sursaturé se décompose entre 500°C (773 K) et la température ambiante. Nous comparons nos observations avec celles qui ont été publiées antérieurement, et nous proposons une nomenclature cohérente des phases métastables. Nous avons mis en évidence la formation d'une phase métastable équiaxe, antérieure aux zones GP en plaquettes bien connues. Nous analysons également la suite des précipitations en fonction de la température et de la méthode de trempe. Nous discutons des résultats à partir de la théorie de la germination.

Zusammenfassung—Wir fassen hier die Formen und die Effekte verschiedener metastabiler Phasen, die während des Zerfalles einer übersättigten Cu–2 Gew.-% Be-Legierung zwischen 500°C (773 K) und Raumtemperatur auftreten, auf die Elektronenbeugung zusammen. Die Beobachtungen werden mit früheren verglichen; eine konsistente Bezeichnung der metastabilen Phasen wird angegeben. Es wurde gefunden, daß sich eine gleichachsige metastabile Phase vor der wohlbekannten plattenförmigen Guinier-Preston-Ausscheidung bildet. Außerdem wird die Folge der Ausscheidungsbildung in Abhängigkeit von Temperatur und Abschreckmethode angegeben. Die Ergebnisse werden mit der Keimbildungstheorie diskutiert.

INTRODUCTION

The precipitation sequence in Cu–Be alloys has been extensively studied. There exists a wide variety of interpretations in the literature as to the morphology, crystallography and habit planes of the several intermediate (metastable) phases which form prior to the equilibrium γ phase. In this paper we will demonstrate that at large enough undercoolings four metastable phases form prior to the formation of the equilibrium γ phase. Furthermore, we will show that the morphology and sequence of precipitation depends not only on the aging temperature, but also on whether the alloy is quenched directly to the aging temperature (from the solution temperature) or if it is quenched to room temperature prior to aging. We shall denote these two kinds of quenches 'down quench' and 'up quench,' respectively.

To avoid confusion over the terms given to the various phases, we shall first present diffraction patterns and micrographs of each of the precipitates that we observe to form. The various habit planes will be delineated, and the designation of the phases will be compared to those in the literature. The precipitation sequence will then be discussed in terms of nucleation theory.

EXPERIMENTAL PROCEDURE

High purity Cu–2% Be alloys were solution treated in a tube furnace, with an inert atmosphere, for 3 h at 800°C (1073 K). Samples were directly quenched to the aging temperature (down quenched) or quenched to water at room temperature and then reheated to the aging temperature (up quenched). The aging temperatures employed varied from room temperature 23°C (296 K) to 500°C (773 K) and were performed in salt baths.

Discs 3 mm diameter were obtained from the heat treated samples and electropolished by means of the double jet electropolishing technique. The solution used consisted of 1/3 nitric acid and 2/3 methanol at −30°C (243 K). This resulted in thin foils suitable for TEM observation.

Bright-field, dark-field and weak beam microscopy were performed. Weak beam images were obtained on the (022) matrix reflection with the $\mathbf{g}$–$3\mathbf{g}$ condition being satisfied. This resulted in values of $\mathbf{s} \approx 2 \times 10^{-2}\,A^{-1}$.

The transmission electron microscope employed was a JEM 100B equipped with a double tilt stage capable of $\pm 36°$ on one axis and $\pm 60°$ on a perpendicular axis.

RESULTS AND DISCUSSION

A. Precipitate characteristics

Several investigators [1–3] have found that three metastable phases form prior to the equilibrium γ phase in Cu–Be alloys with compositions in the range 1–2w/o Be. By analogy with the well known Al–Cu system these phases are usually denoted as G.P., γ'' and γ', in order of increasing stability. However there is some confusion in the literature on the designations of these phases. Thus, the morphology of these phases and characteristic diffraction patterns will first be presented and discussed.

1. G.P. Zones. Since the early work of Guinier and Jacquet [4] most investigators agree that plate-like monolayers of Be atoms form on the {100} planes of the Cu-rich matrix at temperatures below 430°C (703 K). This phase has been characterized by both X-ray diffraction [4–6] and electron microscopy [7–12]. The characteristic continuous ⟨100⟩ streaks in the electron diffraction patterns are well known and are shown in Fig. 1a. Dark field electron microscopy performed at a position along one of the ⟨100⟩* streaks give rise to an image of the zones (Fig. 1b). They are seen to be about 100 Å in diameter and 10 Å thick, though the thickness is really a measure of the extent of the strain field which surrounds the Be monolayer.

These G.P. zones are not, however, the least stable of the metastable phases in the Cu–Be system. At room temperature equiaxed Be enriched zones have

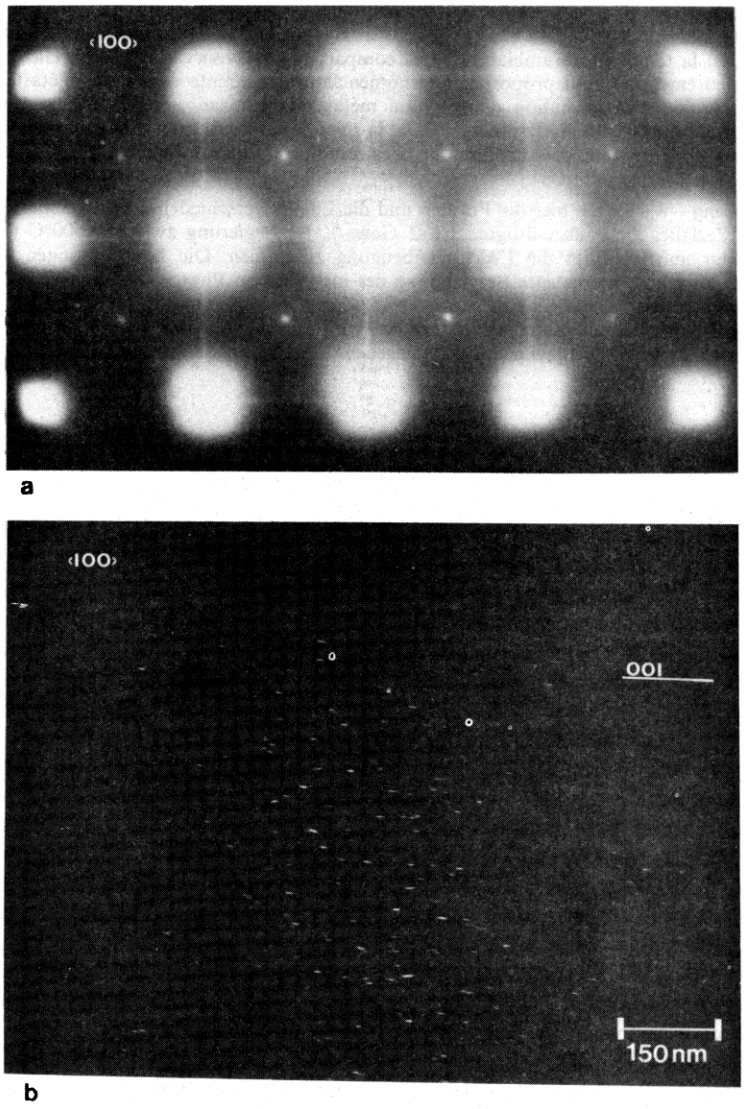

Fig. 1. GP zones. (a) SADP of a sample DQ to 350°C and aged for 5 min. Zone axis [100]. Notice the streaks due to GP zones along the ⟨100⟩ directions. (b) DF obtained by imaging the [001] streak. Notice that GP zones appear as bright lines, along the (001) planes.

been observed to precede their formation. This is discussed later in this paper.

2. γ'' Phase. Further aging of DQ samples at 300°C (633 K) or below, results in the 'bunching up' of the $\langle 100\rangle^*$ streaks near the $\pm\frac{2}{3}\{200\}^*$ reciprocal lattice positions (see Figure 2a)). An increase in intensity near the $\pm\frac{1}{3}\{200\}^*$ positions is also observable, but these are usually attributed to double diffraction from the $\pm\{200\}^*$ reflections [2]. A dark field photograph taken with axial illumination from one of the $\frac{2}{3}\{200\}^*$ intensity maxima is shown in Fig. 2b. It can be seen that the phase also has a habit plane $\{100\}_\alpha$ and that the plates line up along the traces of the $\{110\}_\alpha$ planes.

The elucidation of the structure of this phase has been very difficult.

Geisler *et al.* [13] observed a phase with $\{100\}$ habit planes to form after the G.P. zones. Based on X-ray diffraction results they concluded that the crystal structure of γ'' was body centered monoclinic with $\beta = 85° \cdot 25'$ and $a = b = 2.54$ Å and $c = 3.24$ Å. They proposed the crystallographic orientation relationship to be $(\bar{1}\bar{1}1)_\alpha \parallel (\bar{1}11)_{\gamma''}$ and $[\bar{1}10]_\alpha \parallel [001]_{\gamma''}$.

Yamamoto and Murakami [9] proposed that the γ'' phase was an 'ordered phase' with a lattice parameter approximately three times that of the copper-rich solid solution. This was based on the notion that the $\frac{1}{3}\{200\}_\alpha$ spots were true reflections. No discussion of the possibility of them being due to double diffraction was included in their paper.

Shimizu *et al.* [2] attribute the $\frac{1}{3}\{200\}_\alpha$ reflections to double diffraction. The $\frac{2}{3}\{200\}_\alpha$ reflection ($d \approx 2.9$Å) was attributed to the piling up of G.P. zones on every other $\{100\}_\alpha$ plane. Not accounting for any accommodation by strain, the γ'' phase would therefore have a body centered tetragonal structure with:

$$a_{\gamma''} = \frac{a_\alpha}{\sqrt{2}} \approx 2.53\ \text{Å}$$

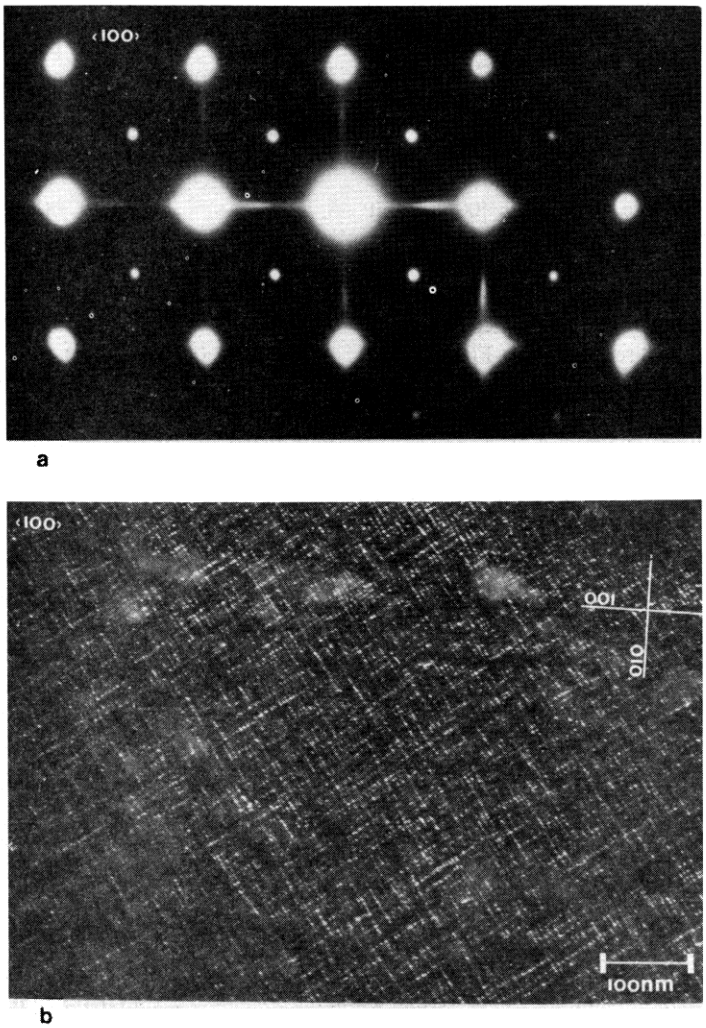

Fig. 2. γ'' precipitates. (a) SADP of a sample DQ to 250°C and aged for 5 min. Zone axis [100]. Notice an increase in intensity around 2/3(002) in the $\langle 100\rangle$ directions. (b) DF obtained by imaging the maximum in intensity at 2/3(002). Notice the alignment of γ'' precipitate along the traces of the $\{110\}$ planes.

and

$$c_{\gamma''} = 2.9\,\text{Å}$$

with the crystallographic relationships:

$$(001)_{\gamma''} \parallel (001)_\alpha$$
$$[100]_{\gamma''} \parallel [1\bar{1}0]_\alpha$$

It is very difficult, however, to distinguish between the model of Geisler *et al.* [13] and Shimuzu *et al.* [2]. The electron diffraction 'reflections' of the γ'' are elongated due to shape effects. This makes it impossible for TEM results to rule out a small monoclinic distortion. Furthermore, the difference in c parameter can be attributed to the fact that the former investigators made their observation earlier in the transformation process.

3. γ' Phase. With further aging the $\frac{2}{3}\{200\}^*$ reflections fan out into an 'arrowhead'-like shape (Fig. 3a). The angle between the [001]* and the streaks in the 'arrowhead' is about 36° in the [110] zone axis. Dark field imaging of the 'arrowhead' shows the phase to have its habit plane distinct from that of the γ'' phase. Trace analysis from zone axis near the [011] showed that the habit planes are the $\{112\}_\alpha$ planes.

This phase has been designated γ by some authors [2] and γ' by others [13]. Whatever it is termed, it is not the stable phase (γ) and it is more stable than those metastable phases with $\{001\}_\alpha$ habit planes (G.P., γ''). For this reason, in analogy with the Al–Cu system we prefer to call the phase γ'.

The 'arrowhead' reflections continuously changes into more or less discrete reflections which are elongated along the $[113]_\alpha$ directions (see Fig. 3b–d).† This change in habit plane is not accompanied by a change in crystal structure. Hence the phase shown in Figs 3b and 3d is still designated γ'.

This phase is tetragonal with a = 2.70 Å and c = 2.56 Å according to the SADP of Fig. 4a; Fig. 4c is the DF of this phase. The habit plane of this phase seems to evolve continuously from the $\{112\}_\alpha$ planes to the $\{113\}_\alpha$ planes. Geisler *et al.* [13] reported a phase termed γ' which had a = 2.79 Å and c = 2.54 Å with the following crystallographic orientation with the parent:

$$(\bar{1}\bar{1}2)_\alpha \parallel (\bar{1}20)_{\gamma'}$$
$$[\bar{1}10]_\alpha \parallel [001]_{\gamma'}$$

Shimuzu *et al.* [2] and Bonfield and Edwards [14–16] reported a cubic phase which they termed γ and γ' respectively, with a = 2.7 Å and the following orientation with the parent:

$$(\bar{1}13)_\alpha \parallel (130)_{\gamma'}$$
$$[110]_\alpha \parallel [001]_{\gamma'}$$

† The γ' reflections shown in Fig. 3(a) and (b) are only observed along one of the $\langle 100\rangle^*$ directions. This preferential formation of one variant of a tetragonal phase we term the 'self-stress orienting phenomenon,' and is the topic of a subsequent publication.

Our results indicate that the γ' phase at the early stages has the $(112)_\alpha$ habit plane as reported by Geisler *et al.* [13]. Nevertheless, as the γ' precipitates continue to grow, the habit plane changes from the $\{112\}_\alpha$ to the $\{113\}_\alpha$ planes and the c-axis expands until the value 2.7 Å is approached. In this case, the crystallographic orientation relationship proposed by Shimuzu *et al.* [2] and by Bonfield and Edwards [14–16] was observed. It was also observed that the precipitation sequence of samples DQ to 350°C and 400°C (623 and 673 K) was of the form:

$$\alpha_{ss} \rightarrow \alpha + \text{G.P.} \rightarrow \alpha + \gamma'$$

that is, the γ'' phase did not form. Figure 4d shows the DF of a sample in which G.P. zones and γ' precipitates are present. The SADP of the micrograph is shown in Fig. 3d. This anomalous precipitation sequence will be discussed in the following section. The γ' phase also forms as a grain boundary reaction with the same orientation with the matrix as shown by Bonfield and Edwards [15]; see Fig. 4e.

4. The γ Phase. The equilibrium phase (γ) has the B2 structure and lattice parameter a = 2.7 Å [13]. During the course of this investigation two crystallographic orientation relationships were observed.

When the γ phase formed after the γ' phase, the Bain orientation was observed. That is,

$$(110)_\alpha \parallel (100)_\gamma$$
$$[100]_\alpha \parallel [100]_\gamma$$

A selected area diffraction pattern (SADP) of this phase is shown and indexed in Fig. 5a and b; the morphology of the γ phase with the Bain orientation is shown in Fig. 5c.

When the γ phase forms directly from the supersaturated α matrix, the Kurdjumov-Sachs orientation was observed, i.e.,

$$(111)_\alpha \parallel (101)_\gamma$$
$$[1\bar{1}0]_\alpha \parallel [11\bar{1}]_\gamma$$

A SADP of this phase is shown in Figure 6a. The morphology of the precipitates giving rise to the extra reflections in the SADP of Fig. 6a is shown in Fig. 6c. Previous to these results the crystallographic orientation of the γ phase with respect to the matrix had been suggested to be:

$$(001)_\alpha \parallel (001)_\gamma$$
$$[100]_\alpha \parallel [110]_\gamma$$

according to Guy [17]

and

$$(\bar{1}\bar{1}1)_\alpha \parallel (\bar{1}10)_\gamma$$
$$[\bar{1}10]_\alpha \parallel [001]_\gamma$$

according to Geisler *et al.* [13]

5. Equiaxed Zones. As mentioned earlier, we have observed a precursor to the plate-like G.P. zones in

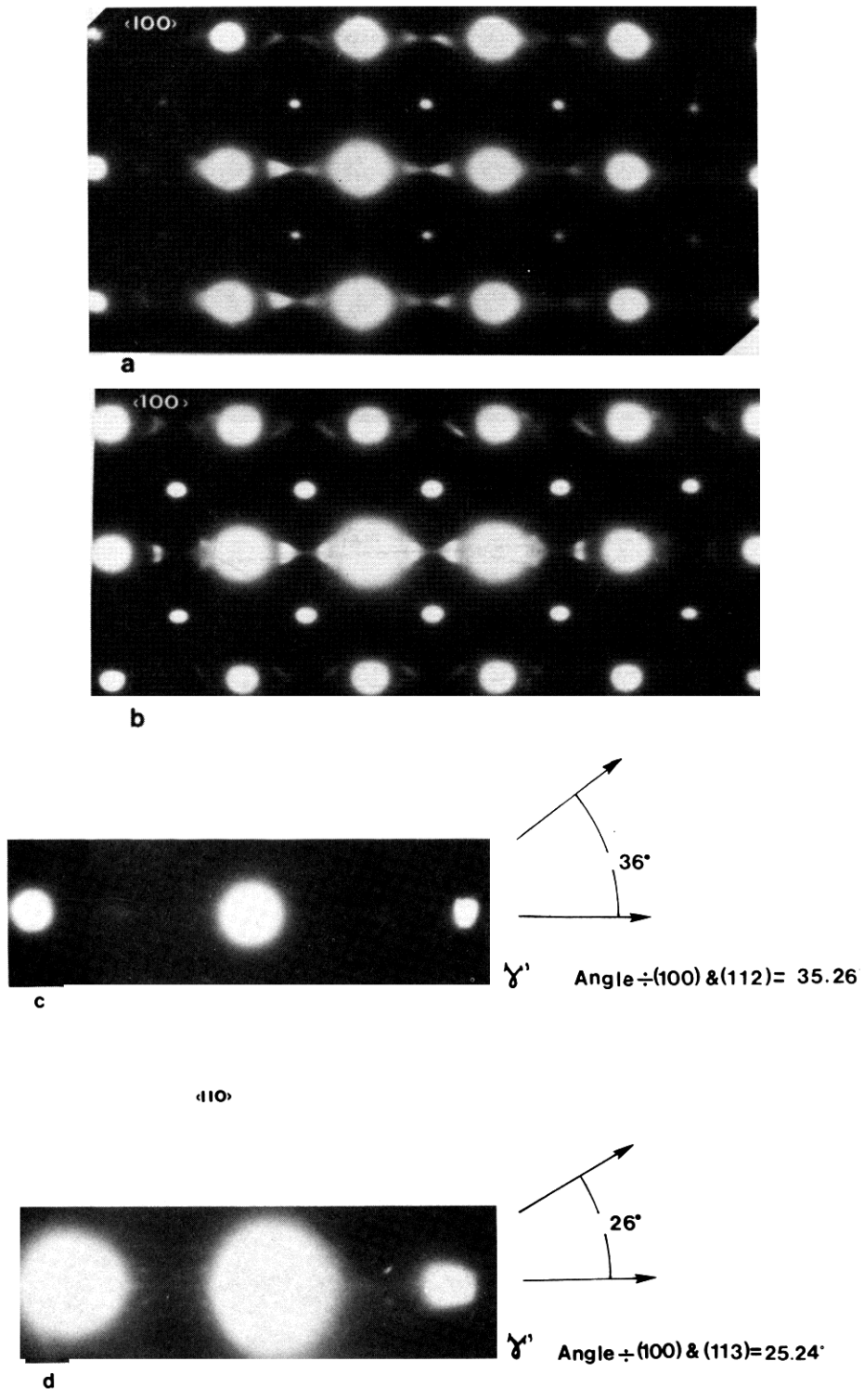

Fig. 3. γ' precipitate. (a) SADP of a sample DQ to 350°C and aged for 7 min. (b) SADP of a sample DQ to 350°C and aged for 30 min. Notice that the 'arrowhead'-like reflections evolve into discrete reflections. Zone axis is [100]. (c) SADP of a sample exhibiting 'arrowhead'-like reflections. The angle between the streaks and the [001] measured from SADP's is 36°. n.b. angle between (100) and (112) in cubic structures is 35.26°. (d) SADP of a sample exhibiting γ' reflections. The angle measured from the SADP is 26°. n.b. angle between (100) and (113) in cubic structures is 25.24°. Zone axis is [110] in both (c) and (d).

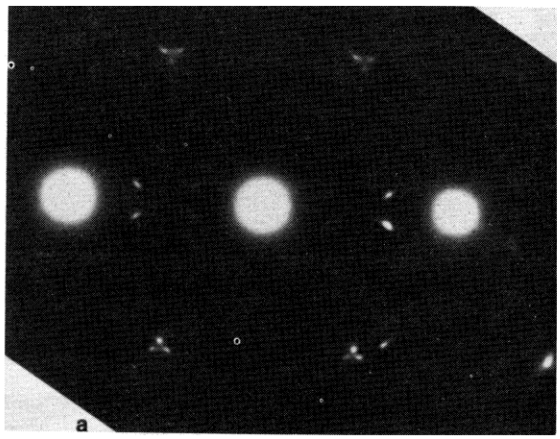
a

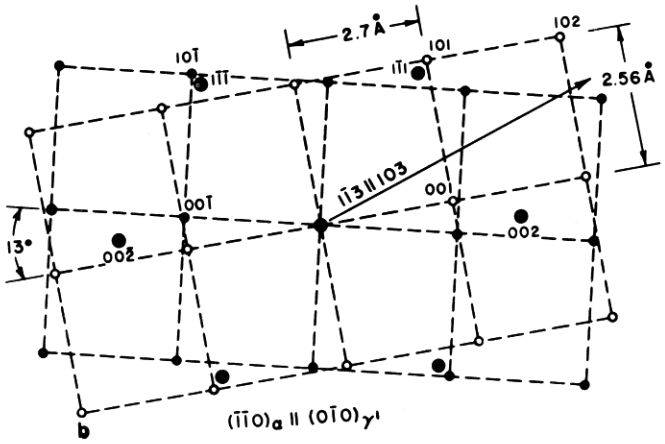
2.7 Å
2.56 Å
10$\bar{1}$
$\bar{1}$11
101
$\bar{1}$11
102
$\bar{1}$13 ∥ 103
00$\bar{1}$
001
13°
00$\bar{2}$
002
b
$(\bar{1}\bar{1}0)_\alpha \parallel (0\bar{1}0)_{\gamma'}$

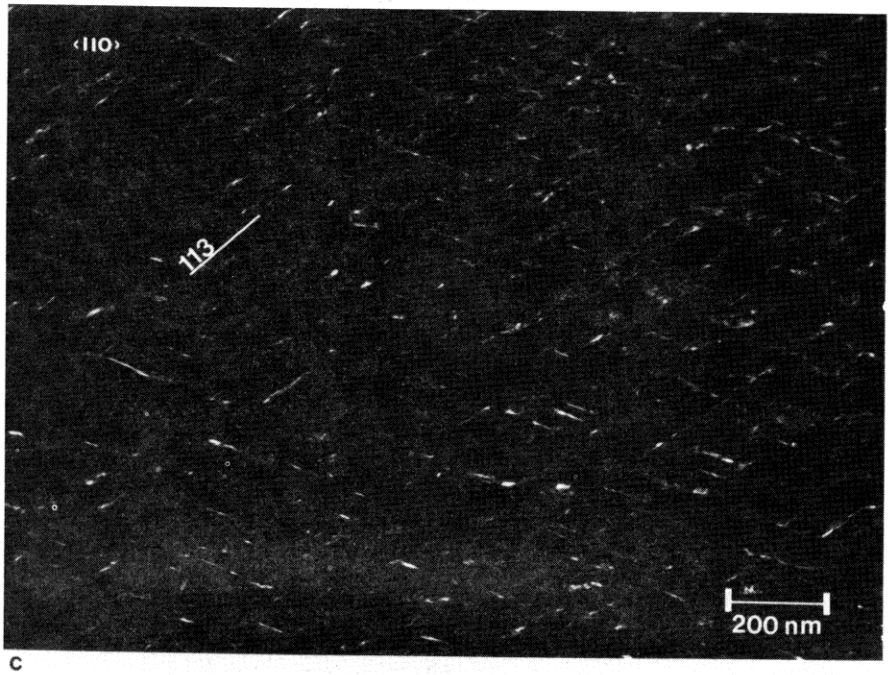
‹110›
113
200 nm
c

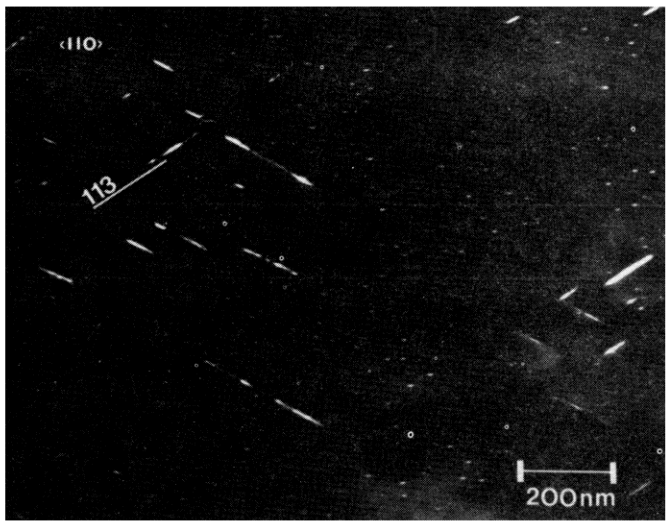

d

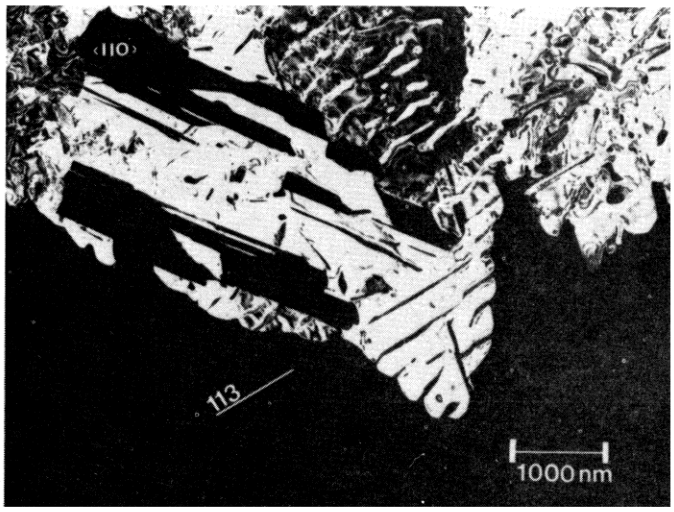

e

Fig. 4. γ' precipitate. (a) SADP of a sample DQ to 410°C for 3 min. (b) Schematic of the previous SADP showing the α parent and the γ' reflections. The orientation of the foil is [110]. (c) DF corresponding to the previous SADP. Notice the (113) habit plane of the γ' phase. (d) DF of a sample DQ to 400°C and aged for 5 min. The DF was obtained by imaging the γ' reflections and the streaks due to GP zones. Notice that GP zones and γ' precipitates are present. (e) (111) matrix DF of a sample DQ to 450°C and aged for 10 min. Notice the γ' precipitates at the tip of the advancing interface of the grain boundary reaction. Zone axis is [110] in both (d) and (e).

this system, when the alloy is aged at room temperature. The precursor phase consists of 'equiaxed clusters" of Be enriched regions, approximately 15–30 Å (1.5–3 nm) in diameter. These clusters can be seen in bright-field as dark 'spots,' but are best observed by weak beam microscopy. Fig. 7a shows the equiaxed clusters (white regions) in an alloy aged 10 min. at room temperature. The corresponding diffraction pattern (Fig. 7b) shows that the platelike G.P. zones are not yet present (lack of the long ⟨100⟩* streaks) but faint, short ⟨110⟩* relrods are present. Conventional bright-field microscopy at this stage of the aging process reveals ⟨110⟩ tweed [11, 12]. Comparison of the weak beam photographs performed with [100]* and [110]* zone axis reveals that the clusters are aligned along the ⟨100⟩ and the ⟨110⟩ directions, respectively.

It is interesting to note that the existence of these equiaxed zones is consistent with the recent theoretical work of Lee, Barnett and Aaronson [18]. They have suggested that if 'f.c.c. Be zones' are elastically harder than an f.c.c. Cu matrix, the zones should have a spherical shape to minimize strain energy. Also, it is well known that if the surface energy is assumed to be isotropic, a sphere minimizes that energy as well. Hence, when Be clusters begin to form in a Cu matrix both surface and strain energy is minimized by the formation of equiaxed or spherical clusters. However,

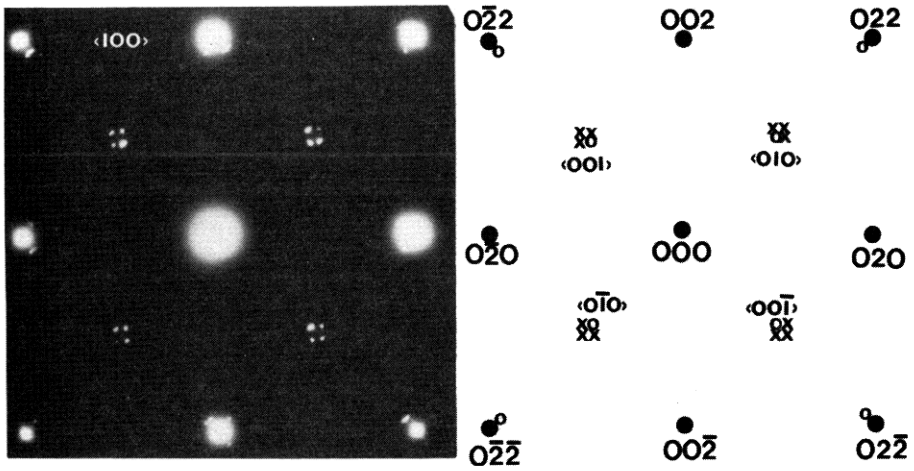

a b

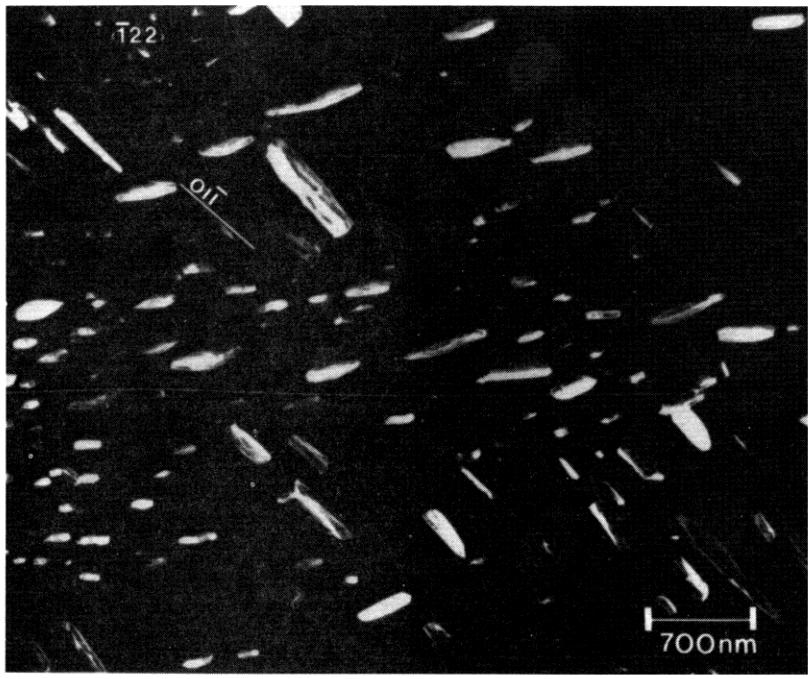

c

Fig. 5. γ precipitates. (a) SADP of a sample DQ to 450°C and aged for 10 min. The SADP was obtained from a region near the original grain boundary, within the regions transformed by the grain boundary reaction. (b) Schematic of the previous SADP showing the matrix and the γ reflections. Zone axis is [100]; 0 = γ reflections, X = double diffraction. (c) DF of the γ phase formed after the γ' phase. Zone axis is [$\bar{1}$22] Notice the (0$\bar{1}$1) habit plane of the precipitates.

the lattice mismatch ($\sim 12\%$) prohibits the growth of these clusters beyond *ca.* 50 Å. The mismatch is such that a plate will then minimize the strain energy, as it is impossible to build up three dimensional coherent particles with such a large mismatch. This is similar to what happens in the Al–Cu case [19] except that there, the change in shape of the solute-enriched clusters occurs via the spinodal mechanism. In Cu–Be, no evidence for spinodal decomposition has been found. Therefore, the plate-like G.P. zones most probably form by a nucleation mechanism in those regions enriched in Be.

B. Precipitation sequence

In systems with several metastable phases it is of interest to document the sequence in which precipitates form at various temperatures. We have observed

the following sequences in the Cu–Be system:

(1) at 400°C (673 K) G.P., γ', γ
(2) at 350°C (623 K) G.P., γ', γ
(3) at 300°C (573 K) G.P., γ'', γ', γ

Following Russell and Aaronson [20] we seek to understand the factors which give rise to this temperature dependent sequence. In particular we wish to explain the absence of γ'' at 400°C and 350°C, even though its solvus lies above that of the G.P. zones.

The rate of nucleation, at steady state, can be expressed as [21]

$$J\alpha N \exp\left(-\frac{\Delta G^*}{kT}\right) \quad (1)$$

where

J = the nucleation rate
N = the number of nucleation sites per unit volume
ΔG^* = the critical activation free energy for the formation of the critical nucleus.

For the nucleation of a disc of radius r and half-thickness c, the ΔG^* is given as:

$$\Delta \dot{G}_i^* \propto \frac{\sigma_{i(1)}\sigma_{i(2)}^2}{(\Delta G_i^V + W_i)^2}$$

where

$\sigma_{i(1)}$ = the surface energy of the flat surface of the i^{th} phase.

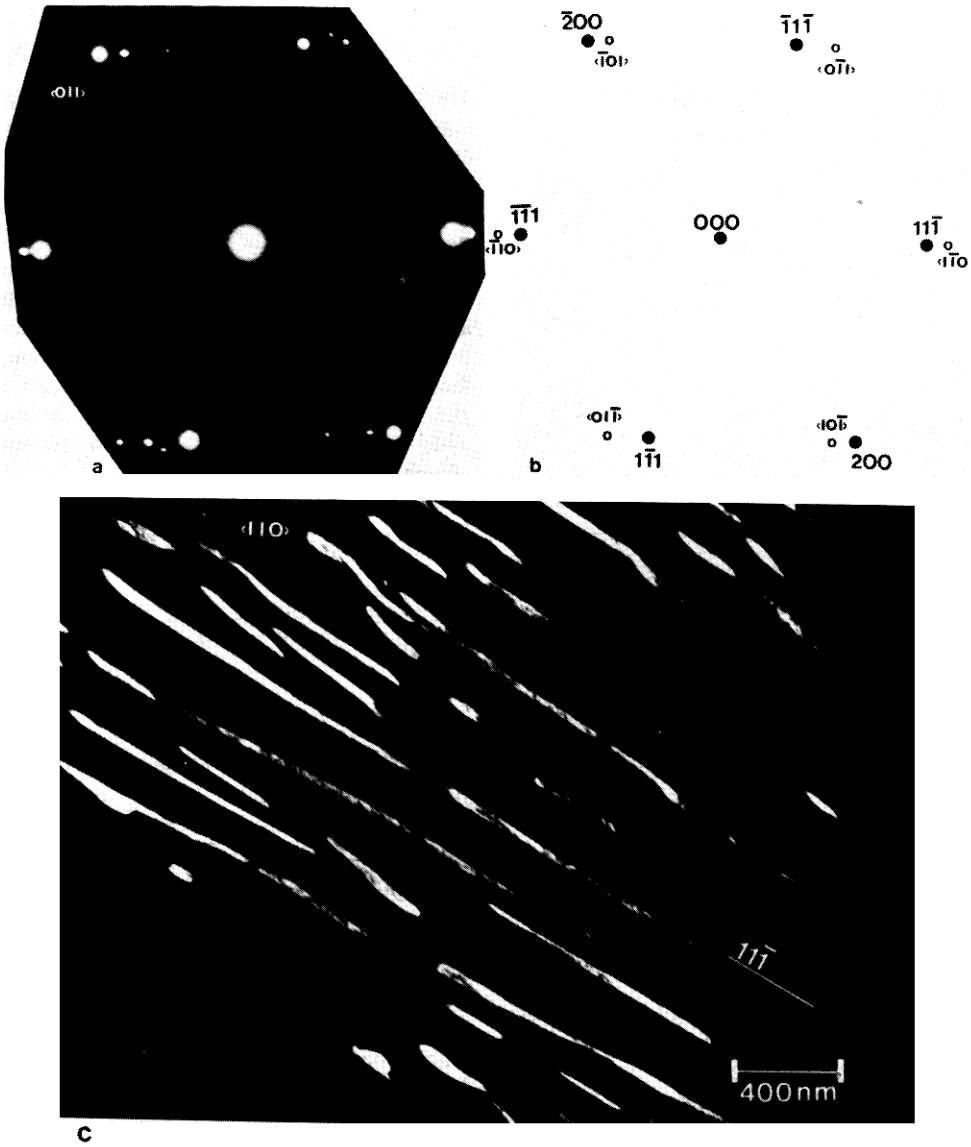

Fig. 6. γ precipitates. (a) SADP of a sample DQ to 500°C and aged for 3 min. Zone axis of matrix is [110]. (b) Schematic of the previous SADP showing the α parent and the γ reflections. The crystallographic orientation relationship between γ precipitates and matrix is the Kurdjumov-Sachs orientation. The extra spots, not indexed, are due to double diffraction. (c) DF of the precipitates formed directly from the supersaturated parent phase. The DF was obtained by imaging the $(1\bar{1}0)$ γ reflection from DP shown in (a) of previous figure. Notice the $(11\bar{1})$ habit plane of the precipitates.

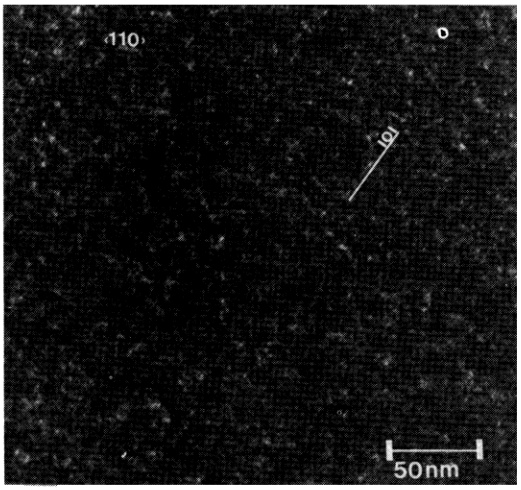

a

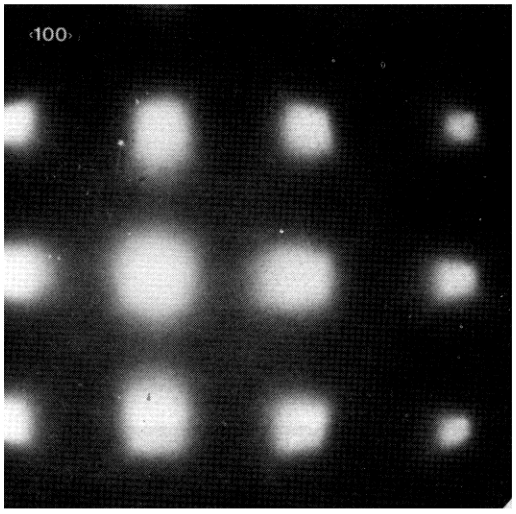

b

Fig. 7. Equiaxed zones. (a) WB micrograph of a sample in the as-quenched condition. Zone axis is [110]. The **g** vector used was $\mathbf{g} = (2\bar{2}0)$ and the $\mathbf{g} - 3\mathbf{g}$ condition was satisfied. Notice the small equiaxed zones *ca.* 1.5 nm. (b) SADP corresponding to the previous sample. The orientation of the foil is [100]. Notice that the ⟨100⟩* streaks due to GP zones are not present.

$\sigma_{i(2)}$ = the surface energy of the edge of the i^{th} phase.

ΔG_i^V = the volume free energy change accompanying the formation of the critical nucleus of the i^{th} phase.

W_i = the volume strain energy change accompanying the formation of a coherent or semicoherent nucleus of the i^{th} phase. For an incoherent phase $W_i = 0$.

From the thermodynamic point of view any of the phases *may* form for which $\Delta G_i^V + W_i < 0$. This is equivalent to saying that the temperature must be below the 'solvus' (be it incoherent or coherent) of a phase if it is to form. However, there exists a large range of temperatures in which *all* the metastable phases *may* form (viz. below the lowest metastable solvus) and the question of importance is which ones *will* form.

If it is assumed that the same sites for nucleation may be utilized by each of the phases, the phase with the lowest ΔG_i^* will be the one which forms fastest. The above stated sequences can be explained as follows:

(*a*) *at 300°C (573 K).* The stated sequence implies:

$$\Delta G^*_{\text{G.P.}} < \Delta G^*_{\gamma''} < \Delta G^*_{\gamma'} \tag{4}$$

or

$$\frac{\sigma_{\text{G.P.}(1)}\sigma^2_{\text{G.P.}(2)}}{(\Delta G^V_{\text{G.P.}} + W_{\text{G.P.}})^2} < \frac{\sigma_{\gamma''(1)}\sigma^2_{\gamma''(2)}}{(\Delta G^V_{\gamma''} + W_{\gamma''})^2} < \frac{\sigma_{\gamma'(1)}\sigma^2_{\gamma'(2)}}{(\Delta G^V_{\gamma'} + W_{\gamma'})^2} \tag{5}$$

These relations are valid because at large supercoolings, the denominators all increase in magnitude and approach similar values. Hence the controlling variables are the surface energies. Clearly the coherent G.P. zones have the lowest surface energy, therefore its value of ΔG_i^* is the lowest. The values $\sigma_{\gamma''(2)}$ and $\sigma_{\gamma'(2)}$ are probably approximately equal because the edges of both phases are incoherent. Thus, the $\sigma_{\gamma''(1)}$ and $\sigma_{\gamma'(1)}$ terms are the important ones in determining the sequence of γ'' and γ'. Since γ'' is coherent on the face we imply $\Delta G^*_{\gamma''} < \Delta G^*_{\gamma'}$. Thus at 300°C (573 K) the sequence of precipitation occurs in increasing order of surface energy, with no phases being skipped [20].

(*b*) *350°C (623 K) and 400°C (673 K).*

$$\Delta G^*_{\text{G.P.}} < \Delta G^*_{\gamma'} < \Delta G'_{\gamma''} \tag{6}$$

or

$$\frac{\sigma_{\text{G.P.}(1)}\sigma^2_{\text{G.P.}(2)}}{(\Delta G^V_{\text{G.P.}} + W_{\text{G.P.}})^2} < \frac{\sigma_{\gamma'(1)}\sigma^2_{\gamma'(2)}}{(\Delta G^V_{\gamma'} + W_{\gamma'})^2} < \frac{\sigma_{\gamma''(1)}\sigma^2_{\gamma''(2)}}{(\Delta G^V_{\gamma''} + W_{\gamma''})^2} \tag{7}$$

The absence of the γ'' phase at 350°C must occur because the denominator for the γ'' decreased to such an extent that it no longer dominated the inequality. In thermodynamic terms: the supersaturation was too small. This did not affect the G.P. zones at these temperatures, however, since the value of $\Delta G^V_{\text{G.P}}$ is about twice that of $\Delta G^V_{\gamma''}$ (see Fig. 9). Nevertheless at temperatures close to the G.P. solvus, G.P. zones would not form for the same reason.

It should be noted that the 'skipping' of a metastable phase in a sequence occurred in this system because the G.P. zones were much richer in solute than the other metastable phases. For example, it would not be possible for γ'' to form without γ' also forming, since for these phases

$$\Delta G^V_{\gamma''} > \Delta G^V_{\gamma'}$$

(viz. closer to zero and hence smaller in absolute magnitude).

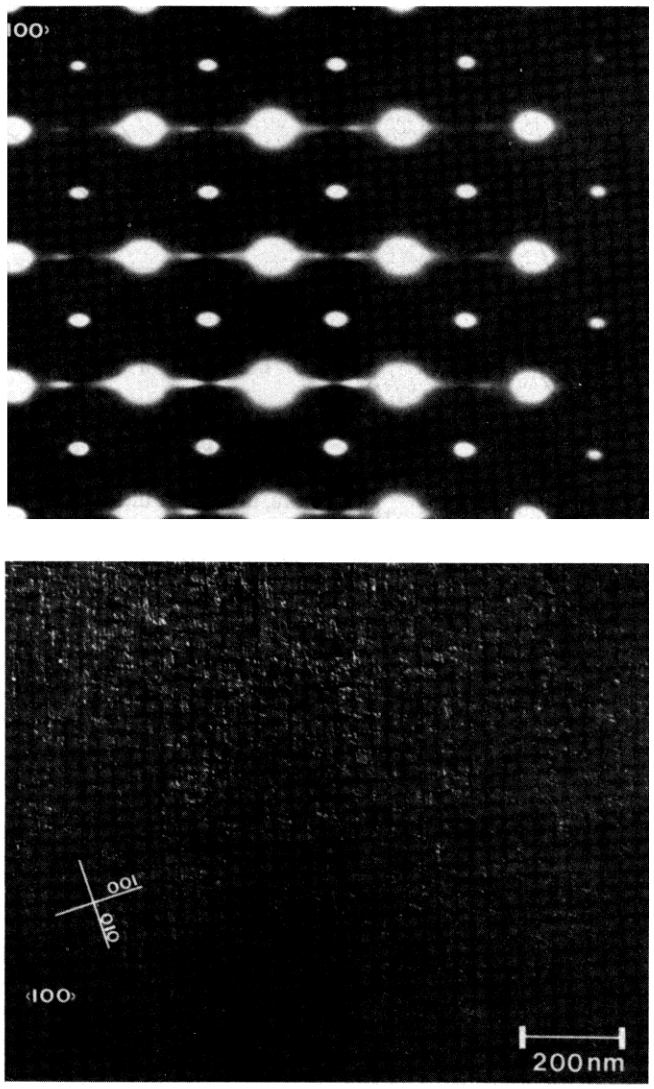

Fig. 8. γ'' precipitates formed in UQ samples. (a) SADP of a sample UQ to 350°C for 5 min. Notice the γ'' reflections. cf. Fig. 2(b). (b) DF corresponding to the previous SADP. Notice the fine dispersion of γ'' precipitates. Zone axis is [100].

C. Down-quenched vs up-quenched alloys

In the past it has been noted by several authors that the kinetics of an isothermal transformation often depends on the temperature–time history immediately preceding the isothermal aging. In this investigation alloys were solutionized at the same temperature, 800°C (1073 K), and quenched to aging temperatures by two paths:

(1) Directly into a bath at the aging temperature (termed 'down-quenched')

(2) Directly into ice water and then up-quenched into a bath at the aging temperature (termed 'up-quenched').

The microstructure and diffraction patterns of two such treatments are shown in Figs 1a,b and 8a,b. The aging temperature was 350°C (623 K) and aging time 5 min. The down-quenched sample has G.P. zones present as indicated by the long continuous $\langle 100 \rangle^*$ streak. The up-quenched sample has mostly γ'' phase present, as indicated by the bunching at $\frac{2}{3}\{200\}$ positions in reciprocal space.

It is apparent that the 'up-quenched' sample has proceeded further along its decomposition path for the same time at the aging temperature. This is best explained by noting that the water-quenched sample existed for some time at a very large supercooling and hence some of the nuclei that would be sub-critical at the aging temperature would be supercritical at room temperature. During the up-quench to the aging temperature these would grow and in effect 'seed' the reaction.

Of greater interest, however, is the fact that γ'' formed in the up-quenched sample, whereas it does

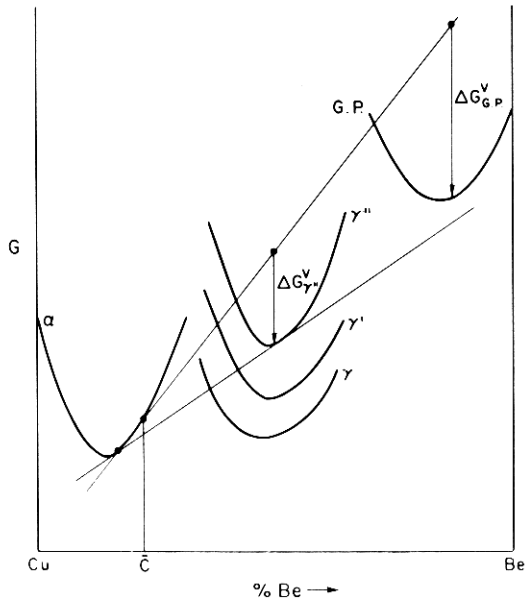

Fig. 9. Schematic of the free energy curves for the various stable and metastable phases present in Cu–Be. Note that $\Delta G^V_{G.P.} > \Delta G^V_{\gamma''}$ for the same matrix composition $\bar{c}$.

not form in the down-quenched sample, for any time. At 350°C (623 K), down-quenched samples first form G.P. zones then γ', followed by γ.

This phenomenon can be explained by postulating that at 350°C (623 K) the γ'' phase can only form directly from the G.P. zones. This is also suggested by the diffraction evidence; viz, the long $\langle 100 \rangle^*$ reciprocal lattice streaks continuously bunch up at the $\frac{2}{3}\{200\}$ positions. We assert, therefore, that at 350°C (623 K) the γ'' phase forms only after the G.P. zones have grown to a certain size. In samples that are down-quenched to the aging temperature the γ' phase forms before the G.P. zones have grown large enough to begin to transform into γ''. In those samples that are quenched to room temperature and then up-quenched to the aging temperature, the TTT curves of the G.P. and γ'' are shifted to the left (because of enhanced vacancy diffusion, quenched in embryo, etc.), allowing the γ'' phase to form. The same phenomenon (viz, the increase in kinetics of γ'' formation) has been observed at temperatures of 300°C (573 K) and 250°C (523 K), although at these temperatures γ'' also forms in down-quenched specimens. Fig. 10 schematically depicts how the TTT curves shift with prior quench to room temperature. It should be emphasized that the curves are merely a *schematic*, showing only the relative positions of the various TTT start curves.

Thus the kinetics of transformation depend strongly on the type of quench given to the sample. The microstructure also is dependent, both in phase distribution (more copious precipitation in those samples quenched to room temperature) and phase identity (e.g., γ'' can only form if the sample is quenched to room temperature). This implies that the

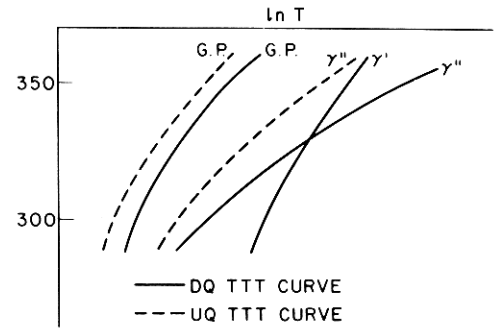

Fig. 10. Schematic TTT curves of G.P. zones, γ'' and γ' in Cu–Be, shown as a function of the type of quench.

resulting properties (e.g., hardness, resistivity) of the alloy will also vary with the kind of quench. Therefore, in reading the literature in this system (as well as many others like it) one must be careful to ascertain the kind of quench used to the aging temperature if he is to compare the results of various authors.

CONCLUSIONS

1. At large enough supercoolings, four metastable phases form prior to the equilibrium γ phase.
2. Beryllium equiaxed clusters form prior to the plate-like G.P. zones.
3. The γ' phase first forms with a $\{112\}_\alpha$ habit plane, but later changes its habit plane to the $\{113\}_\alpha$. Accompanying this change in habit plane is a change in the c/a ratio.
4. Two crystallographic orientation relationships have been observed for the γ phase. When γ forms after the γ' phase, the Bain relation is observed; when γ forms directly from the supersaturated solid solution, the Kurdjumov-Sachs relation is observed.

Acknowledgements—We would like to thank Lee E. Tanner for supplying us with the alloy used herein and for several helpful discussions. Also, Professor A. G. Khachaturyan is to be thanked for several stimulating discussions on the crystallographic aspects of habit planes. R. J. Rioja was supported by a grant from CONACYT (Mexico) and D. E. Laughlin was supported by grants from the National Science Foundation (DMR 76-22353 and DMR 78-05723). Support from the Materials Research Laboratory Section, Division of Materials Research, National Science Foundation, through use of central research facilities is gratefully acknowledged.

REFERENCES

1. Z. Henmi and T. Nagai, *Trans. Jap. Inst. Metals* **10,** 166 (1969).
2. K. Shimizu, Y. Mikami, H. Mitani and K. Otsuka, *Trans. Jap. Inst. Metals* **12,** No. 3, 206 (1971).
3. S. Yamamoto, M. Matsui and Y. Murakami, *Trans. Jap. Inst. Metals* **12,** 159 (1971).
4. A. Guinier and P. Jacquet, *Compt. Rendu.* **217,** 22 (1943); A. Guinier and P. Jacquet, *Rev. Metall.* **41,** 1 (1944).

5. Yu. D. Tyapkin and A. V. Gavrilova, *Sov. Phys. Crystallogr.* **9,** 166 (1964).
6. Yu. D. Tyapkin, *Sov. Phys. Crystallog.* **10,** 418 (1966).
7. I. Pfeiffer, *Z. Metallk.* **56,** 465 (1965).
8. T. Kainuma and R. Watanabe, *J. Jap. Inst. Metall.* **35,** 1126 (1971).
9. S. Yamamoto and Y. Murakami, *Mem. Fac. Engng.* University Kyoto, **31,** 576 (1969).
10. P. Wilkes and M. M. Jackson, *Metall. Sci. J.* **3,** 130 (1969).
11. L. E. Tanner, *Phil. Mag.* **14,** 111 (1966).
12. V. A. Phillips and L. E. Tanner, *Acta Metall.* **21,** 441 (1973).
13. A. H. Geisler, J. Mallery and F. E. Steigert, *J. Metals* **4,** 307 (1952).
14. W. Bonfield and B. C. Edwards: *J. Mater. Sci.* **9,** 398 (1974).
15. *Idem, ibid,* 409 (1974).
16. *Idem, ibid,* 415 (1974).
17. A. G. Guy, C. S. Barrett and R. F. Mehl, *Trans. AIME* **175,** 216 (1948).
18. J. K. Lee D. M. Barnett and H. I. Aaronson, *Metall. Trans.* **8,** 963 (1977).
19. R. J. Rioja and D. E. Laughlin, *Metall. Trans.* **8A,** 1257 (1977).
20. K. C. Russell and H. I. Aaronson, *J. Mater. Sci.* **10,** 1991 (1975).
21. J. W. Christian, *The Theory of Transformations in Metals and Alloys,* Part I, 2nd edn, Pergamon Press (1975).